Orientational Dynamics in Supercooled Liquids near T_c and Comparison with Ideal Mode-Coupling Theory

G. Hinze, David D. Brace, S. D. Gottke, and M. D. Fayer

Department of Chemistry, Stanford University, Stanford, California 94305

(Received 4 August 1999)

Orientational dynamics in supercooled salol and ortho-terphenyl were measured near their critical temperatures, T_c, with optical Kerr effect experiments spanning a very broad range of times. Above T_c, the decays are shown to be in excellent agreement with the master curve predicted by ideal mode-coupling theory when higher order terms are included. Between the critical decay and the von Schweidler power laws, the intermediate time range of the data can be modeled by a power law. This intermediate power law, located at $2 < t < 10$ ps to 500 ps (depending on temperature), shows a significant temperature dependence with a power law exponent of ~ -1 below T_c.

Dynamics in supercooled liquids occur over a very broad range of times. Although the molecular structures of glass forming liquids can be quite different, a general description of supercooled liquid dynamics, along the lines of mode-coupling theory (MCT) [1,2], seems to be applicable to most of them. Quantitative predictions of the MCT have triggered many recent experiments [2,3]. MCT describes density fluctuations, i.e., the density-density correlation function, $\phi_q(t)$. The time dependences of correlation functions that describe liquid properties that are coupled to the density are taken to be similar to $\phi_q(t)$ near T_c [1,2]. Therefore, a variety of experiments, e.g., light scattering [4–8] and neutron scattering [9–12], have been used to address the validity of MCT. Most of the data were taken in the frequency domain, since adequate experimental techniques in the time domain capable of covering a large range in time have been lacking. The exception is concentrated colloidal suspensions, where time domain data have permitted a detailed comparison to MCT [13].

At short times (fast β regime), dynamics attributed to the cage effect determine the shape of ϕ_q. Close to the mode-coupling transition temperature, T_c, the long time tail of the β regime is characterized, *to first order,* by a power law decay, the critical decay law, given as [1,2]

$$\phi_q(t) = f_q^c + |\sigma|^{1/2} h_q \left(\frac{t}{t_\sigma}\right)^{-a}, \qquad (1)$$

where t_σ denotes a rescaling time (discussed further below), and σ is the separation parameter determined by $\sigma = (T_c - T)/T_c$. The anomalous exponent a, $0 \leq a \leq 0.395$, and t_σ should be the same for all observables which couple to the density [1]. For $T > T_c$, the decay of $\phi(t)$ from the plateau f_q^c towards zero occurs, *in first order,* via another power law, the von Schweidler law:

$$\phi_q(t) = f_q^c - |\sigma|^{1/2} h_q B \left(\frac{t}{t_\sigma}\right)^{b}, \qquad B > 0, \quad (2)$$

which describes the onset of structural relaxation, α processes. At very long times, the decay of the α processes is described by a stretched exponential or an exponential

with the time constant τ_α. Both exponents, a and b, are related to the system dependent exponent parameter λ via

$$\lambda = \Gamma^2(1 - a)/\Gamma(1 - 2a) = \Gamma^2(1 + b)/\Gamma(1 + 2b), \qquad (3)$$

where $\Gamma(x)$ is the gamma function. This relationship has been the subject of several recent studies using, e.g., light-scattering techniques [4,5].

Time domain data on salol (phenyl salicylate) and OTP (ortho-terphenyl) were taken using optical Kerr effect (OKE) spectroscopy [14–16]. Details of the experiments will be given subsequently [17]. With an ultrashort pump pulse (fs-ps), a time-dependent optical anisotropy is created, which is monitored via a heterodyne detected (HD) probe pulse with a variable time delay. The HD-OKE experiment measures the system's impulse response function. Kinoshita *et al.* [18] compared HD-OKE with high resolution light-scattering spectra and found excellent agreement. Furthermore, experimental artifacts of the type recently discovered in light-scattering experiments [19,20] do not occur in the HD-OKE experiment. The methods for the analysis of HD-OKE data have been reported in detail [21]. The imaginary part of the Fourier transform of the HD-OKE signal is proportional to data obtained from depolarized light scattering [18].

To observe the full range of liquid dynamics, at each temperature several sets of experiments were performed with different pulse lengths and delays. For times $t < 600$ ps, a mode-locked 5 kHz Ti:sapphire laser/regenerative amplifier system was used ($\lambda = 800$ nm for both pump and probe). The pulse duration was lengthened from 75 to 2000 fs to improve signal-to-noise ratios for the longer time scale experiments. For even longer times, a cavity dumped mode-locked and Q-switched Nd:YAG laser (~ 70 ps pulses) was used for both pump ($\lambda = 1064$ nm) and probe pulses ($\lambda = 532$ nm). The Nd:YAG system covers times out to 12 ns with a delay line. For longer times ($t > 10$ ns), a cw diode laser was used for probing, and a fast digitizer (2 ns) recorded the data. The scans taken over various time ranges always overlapped

substantially permitting the data sets to be merged by adjusting only their relative amplitudes. Great care was taken, and innumerable tests were made, to assure that the data sets could be combined without error or ambiguity.

Salol and OTP samples were made by vacuum distillation into glass cuvettes. The temperature was regulated using a constant flow cryostat or closed cycle refrigerator, which controlled the temperature to ±0.1 K.

A detailed analysis of the full time dependence of the data will be presented subsequently [17,22]. Here, we focus on the intermediate time regime of the impulse response function (1 ps $< t <$ 10 ns) which corresponds in the frequency domain to the region around minimum in the susceptibility, χ''. Figure 1 displays the salol HD-OKE signal between 247 and 290 K on a logarithmic plot. $T_c \cong 257$ K [4,14,23]. Also shown in Fig. 1 is a plot of t^{-1} (dashed line) as an aid to the eye. The highest temperature curves display the dynamics out to the longest time scale (α relaxation, stretched exponentials). For all temperatures, the full span of the decays was measured and used in the analysis of the data. For the lower temperature data sets, only the relatively short time behavior is shown since this is the focus here. At times shorter than the stretched exponential part of the decay, all of the decays display a power law behavior. This power law, the von Schweidler region in the MCT, can be seen in Fig. 1 most clearly in the intermediate temperature data. Within experimental error, at all temperatures, the exponents for the von Schweidler power law [b in Eq. (2)] are identical. The value, averaged over all temperatures, is $b = 0.59$, which is in accord with light-scattering experiments [4].
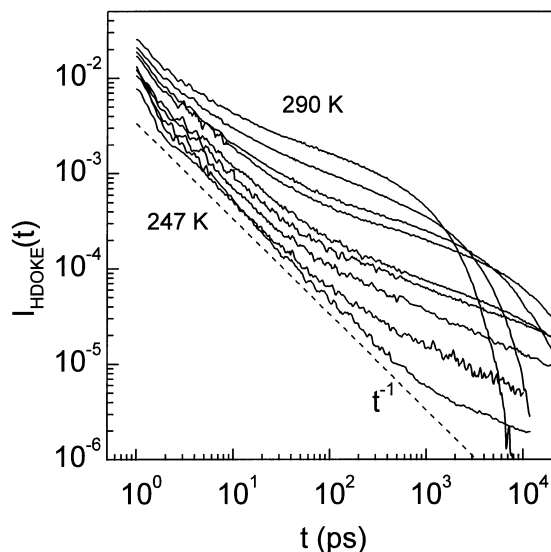

FIG. 1. The HD-OKE signal from salol is plotted vs time for several temperatures: 247, 250, 253, 257, 261, 266, 270, 280, and 290 K (bottom to top). The data are scaled, $I_{HDOKE}(t = 0) = 1$. The data appear to be a power law at intermediate times. This can be seen most clearly in the $T = 247$ K data, where the intermediate power law span is $\sim2 \le t \le \sim500$ ps. The dashed line is a plot of t^{-1} as an aid to the eye.

Analyzing the data at short times with another power law, an exponent is found which varies with temperature. Although the time range for these fits is insufficient to determine the shape of the decay, it is noteworthy that, for $T_c < T < T_c + 10$ K, we find an exponent $a \approx 0.3$ [24], which is in accord with $b = 0.59$ and $\lambda = 0.73$ via Eq. (3) [17]. At higher temperatures, the exponent a decreases, while below T_c this exponent increases to 1.3 at 247 K.

In addition to the short time critical decay (fast β process) power law and the long time von Schweidler power law, we observe a substantial region between these that has the appearance of a power law, which will be referred to as the intermediate power law. The intermediate power law can be seen most clearly in Fig. 1 in the low temperature curves. At 247 K, it extends from $t > 2$ ps up to ~500 ps. Comparison of this curve to the t^{-1} line shows that the data are $\sim t^{-1}$. At 290 K, the intermediate power law exponent is ~-0.6, and the exponent becomes progressively more negative as the temperature decreases. While at the high temperatures, separating the components of the decays is difficult and somewhat arbitrary, at the lower temperatures, the three different power laws can be readily distinguished.

Ideal MCT predicts a two stage relaxation of $\phi_q(t)$; the stages are separated by a plateau with value f_q^c. For $T > T_c$, structural relaxation leads to the final decay of ϕ_q to zero. Below T_c, $\phi_q = f_q^c$ at long times; i.e., there is no structural relaxation. In real molecular liquids, however, structural relaxation occurs even at temperatures significantly below T_c. In extended MCT, hopping processes are assumed to restore ergodicity below T_c [6,7,25]. Since hopping processes take place at all times, for $T < T_c$, instead of the plateau region defined by $\phi_q = f_q^c$, a slightly decaying process should follow the critical decay.

The impulse response function, measured by the HD-OKE experiments, is proportional to the time derivative of the correlation function. Since we observe a functional form that has the appearance of a power law decay in the plateau region, instead of describing the plateau by a constant, we initially use a heuristic model for the purposes of discussion; i.e.,

$$\phi(t) = f^c\left[2 - \left(\frac{t}{t_\xi}\right)\right]. \qquad (4)$$

t_ξ is a rescaling time. In this heuristic description, for $T \le T_c$, the ideal MCT plateau corresponds to $\xi = 0$, and Eq. (4) reduces to $\phi(t) = f^c$. Since the experimental data are related to the derivative of Eq. (4) for ξ approximately zero, the signal will decay as $\sim t^{-1}$.

In Fig. 2, the temperature dependent exponents ξ are plotted for salol and ortho-terphenyl ($T_c = 290$ K) versus a reduced temperature. Within experimental error, the two liquids display identical temperature dependences. For $T > T_c$, $\xi > 0$. ξ decreases with temperature and, below T_c, becomes ~0, within experimental error. $\xi \cong 0$ corresponds to an almost constant correlation function (the
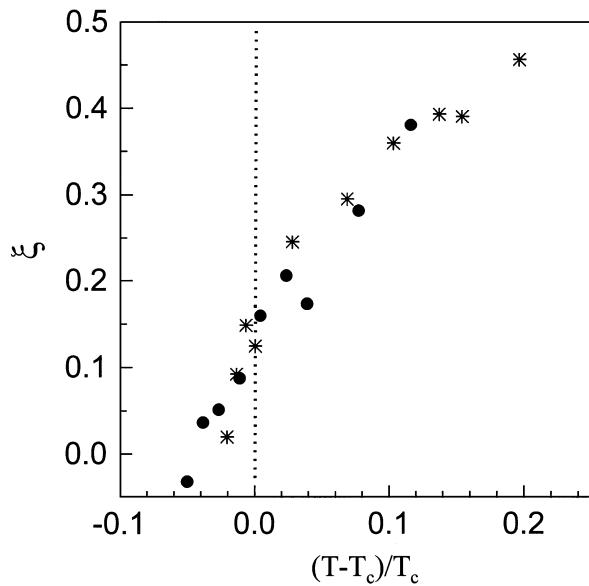
FIG. 2.   The correlation function exponent ξ [Eq. (6)] of the intermediate power law data is plotted versus a reduced temperature for two samples salol ($\bullet$) ($T_c = 257$ K) and orthoterphenyl (*) ($T_c = 290$ K). Within experimental error, the two liquids have the identical temperature dependences of ξ. Slightly below the literature values of T_c, $\xi \approx 0$, which corresponds approximately to a plateau.

"plateau" region) between the critical decay and the von Schweidler regime.

As shown in Figs. 1 and 2, as the temperature decreases, the intermediate power law data span greater time intervals and approach t^{-1}. To examine the intermediate time range quantitatively, it is necessary to go beyond first order in the description of ideal MCT. A quantitative comparison between the data and ideal MCT can be performed by solving the MCT equation of motion to obtain the beta correlator [26] either numerically or by using power law expansions with the appropriate coefficients [27,28]. Here, we employ the power law expansions. With $t_\sigma = t_0|\sigma|^{-1/2a}$, where t_0 is a microscopic time scale, for $t_0 < t \leq t_\sigma$,

$$\phi_q(t) = f_q^c + h_q|\sigma|^{1/2}[(t/t_\sigma)^{-a} - A_1(t/t_\sigma)^a$$
$$+ A_2(t/t_\sigma)^{3a} - A_3(t/t_\sigma)^{5a}$$
$$+ \cdots], \tag{5}$$

and, for $t_\sigma < t \leq \tau_\alpha$,

$$\phi_q(t) = f_q^c + h_q|\sigma|^{1/2}[-B(t/t_\sigma)^b$$
$$+ (B_1/B)(t/t_\sigma)^{-b} + \cdots]. \tag{6}$$

Equations (5) and (6) combine to provide a master curve. Once λ is obtained from experiment, all of the coefficients in Eqs. (5) and (6) are known [27,28]. There are no adjustable parameters in Eqs. (5) and (6). Equation (5) goes over to Eq. (6) at t_σ, and the time axis is scaled by $1/t_\sigma$. Equations (1) and (2) are the first terms in brackets

of Eqs. (5) and (6), respectively. At sufficiently long time, the master curve goes over to a form that is approximately a stretched exponential with time constant $\tau_\alpha \propto |\sigma|^{-\gamma}$ with $\gamma = (1/2a) + (1/2b)$. The long time, α relaxation, portion of the curve will be discussed subsequently [17]. Plots of the master curve show that the fast critical decay power law and the von Schweidler power law are evident at short and long times, respectively. Equation (4) was chosen as a simple model of the intermediate time portion of the master curve because it makes it possible to present a portion of the data, as in Fig. 2, even below T_c, where the master curve is no longer applicable.

Figure 3 displays the salol data compared to the master curve calculations. The curves have been offset on the vertical axis for clarity of presentation. The long time scale, α portions of the calculations have been omitted. Once λ is specified, all of the parameters in Eqs. (5) and (6) are known [27]. For salol, $b = 0.59$, and, therefore,
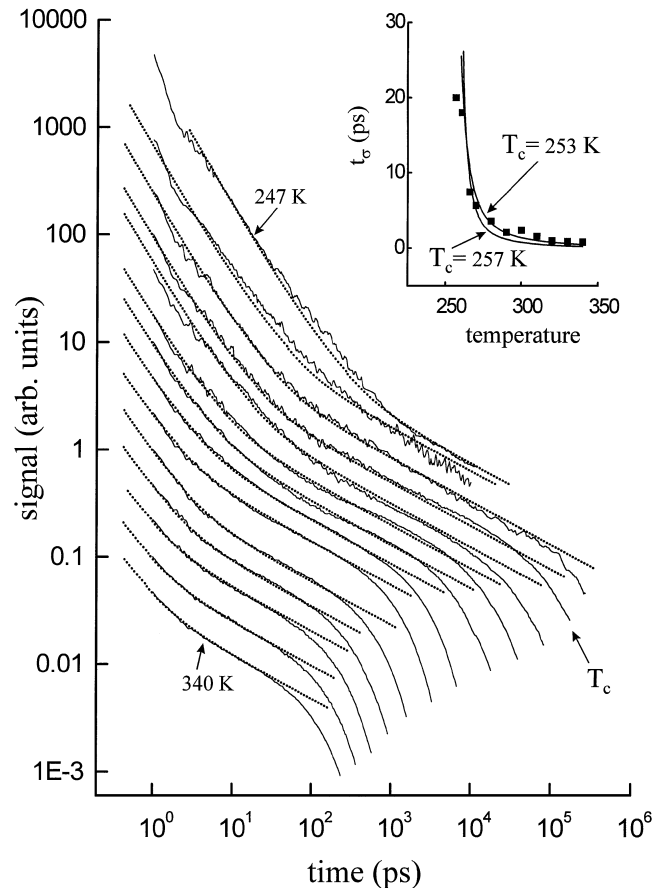

FIG. 3.   The salol data compared to the master curve calculations, Eqs. (5) and (6), predicted by ideal mode-coupling theory. The curves for temperatures (top to bottom) are 247, 250, 253, 257, 261, 266, 270, 280, 290, 300, 310, 320, 330, and 340 K. For temperatures above $T_c \cong 257$ K, the agreement between the predictions of ideal MCT and the data is remarkable. The inset displays the scaling times t_σ used in the data analysis (for the highest 11 temperatures) and the theoretically predicted scaling times (solid curves) for two choices of T_c, 257 and 253 K.

$\lambda = 0.73$. The tabulated expansion coefficients [28] were used without adjustment, only t_σ was adjusted for each temperature to obtain a best agreement. The inset displays the scaling times t_σ used in the data analysis and the theoretically predicted scaling times (solid curve).

Above T_c, the shape of the master curve shows outstanding agreement with the data over the full range of times. The ability of ideal mode coupling theory to reproduce the functional form of the data is remarkable. The scaling times displayed in the inset also show good agreement with the predictions of ideal mode coupling theory until T_c is approached. T_c is known only to within a few degrees. If T_c is taken to be 253 K rather than 257 K, the scaling times predicted by MCT are virtually identical to those found in the data analysis. Thus, within the uncertainty of the value of T_c, at temperatures above T_c ideal MCT can describe the data with no adjustable parameters. Close to and below T_c, it can be seen that the data does not have the same form as the master curve, even with the adjustment of t_σ. Furthermore, in ideal MCT as T_c is approached, the time scaling t_σ goes to infinity. As can be seen in Figs. 1, 2, and 3, the data do not behave as predicted by ideal MCT at or below T_c. Nonetheless, for a range of temperatures above T_c, the ideal MCT master curve does a truly remarkable job of reproducing the data.

The heuristic intermediate power law [Eq. (4)] permits the behavior of the curves to be examined as T goes below T_c. As shown in Fig. 2, salol and OTP have the same behavior, and there is no discontinuity as the temperature drops below T_c. Above T_c, the intermediate power law is a simple, approximate representation of the intermediate region of the master curve. Furthermore, as is evident from Fig. 1, in salol at $T = 247$ K, the intermediate power law is $\sim t^{-1}$ over a broad range of time, implying that the correlation function is almost flat, i.e., $\xi \cong 0$ in Eq. (4). This is somewhat akin to the plateau region predicted by ideal MCT to occur at T_c. It is possible that, below T_c, the virtually flat nature of the correlation function on the intermediate time scale can be explained using extended MCT [6,7,25].

Ultrafast optical Kerr effect relaxation studies on salol and ortho-terphenyl have been performed over a wide range of times and temperatures around T_c. The unprecedented high quality of the time domain data, and the broad ranges of times and signal amplitudes, have made it possible to make a rigorous comparison of the experimental results on molecular glass forming liquids to predictions of ideal MCT. For temperatures above T_c, the data are reproduced very accurately by the ideal MCT master curve. However, there is no discontinuity in the nature of the data as the temperature is taken below T_c. Slightly below the literature values of the T_c, an intermediate power law, $\sim t^{-1}$, is identified which corresponds to an approximately frequency independent susceptibility.

[1] W. Götze and L. Sjögren, Rep. Prog. Phys. **55**, 241 (1992).
[2] W. Götze, J. Phys. Condens. Matter **11**, A1 (1999).
[3] *Proceedings of the Second International Discussion Meeting on Relaxations in Complex Systems,* edited by K. L. Ngai, E. Riande, and G. B. Wright [J. Non-Cryst. Solids **172–174**, 1–435 (1994)]; *Proceedings of the Third International Discussion Meeting on Relaxations in Complex Systems,* edited by K. L. Ngai and E. Riande [J. Non-Cryst. Solids **235–237**, 1–800 (1998)]; *Second Workshop on Non-Equilibrium Phenomena in Super-Cooled Fluids, Glasses, and Amorphous Materials,* edited by M. Giordano, D. Leponini, and M. Tosi [J. Phys. Condens. Matter **11**, A1–A377 (1999)].
[4] G. Li *et al.,* Phys. Rev. A **46**, 3343 (1992).
[5] W. Steffen *et al.,* Phys. Rev. E **49**, 2992 (1994).
[6] H. Z. Cummins *et al.,* Phys. Rev. E **47**, 4223 (1993).
[7] W. M. Du *et al.,* Phys. Rev. E **49**, 2192 (1994).
[8] H. Z. Cummins *et al.,* J. Non-Cryst. Solids **235–237**, 254 (1998).
[9] W. Petry *et al.,* Z. Phys. B **83**, 175 (1991).
[10] M. Kiebel *et al.,* Phys. Rev. B **45**, 10 301 (1992).
[11] J. Wuttke *et al.,* Z. Phys. B **91**, 357 (1993).
[12] A. Tölle *et al.,* Phys. Rev. E **56**, 809 (1997).
[13] W. v. Megen and S. M. Underwood, Phys. Rev. E **49**, 4206 (1994).
[14] R. Torre, P. Bartolini, and R. M. Pick, Phys. Rev. E **57**, 1912 (1998).
[15] S. Palese *et al.,* J. Phys. Chem. **98**, 6308 (1994).
[16] G. Hinze, R. S. Francis, and M. D. Fayer, J. Chem. Phys. **111**, 2710 (1999).
[17] G. Hinze, S. D. Gottke, D. D. Brace, and M. D. Fayer (to be published).
[18] S. Kinoshita *et al.,* Phys. Rev. Lett. **75**, 148 (1995).
[19] J. Gapinski *et al.,* J. Chem. Phys. **110**, 2312 (1999).
[20] H. C. Barshilia *et al.,* Phys. Rev. E **59**, 5625 (1999).
[21] M. Cho *et al.,* J. Chem. Phys. **99**, 2410 (1993).
[22] S. D. Gottke, D. D. Brace, G. Hinze, and M. D. Fayer (to be published).
[23] C. Dreyfus *et al.,* Phys. Rev. Lett. **69**, 3666 (1992).
[24] F. Sciortino and P. Tartaglia, J. Phys. Condens. Matter **11**, A261 (1999).
[25] M. Fuchs *et al.,* J. Phys. Condens. Matter **4**, 7709 (1992).
[26] G. Li, M. Fuchs, W. M. Du, A. Latz, N. J. Tao, J. Hernandez, W. Götze, and H. Z. Cummins, J. Non-Cryst. Solids **172**, 43 (1994).
[27] E. Bartsch, Transp. Theory Stat. Phys. **24**, 1125 (1995).
[28] W. Götze, J. Phys. Condens. Matter **2**, 8485 (1990).